1
Neutron Nuclear Reactions

The physics of nuclear reactors is determined by the transport of neutrons and their interaction with matter within a reactor. The basic neutron nucleus reactions of importance in nuclear reactors and the nuclear data used in reactor physics calculations are described in this chapter.

1.1
Neutron-Induced Nuclear Fission

Stable Nuclides

Short-range attractive nuclear forces acting among nucleons (neutrons and protons) are stronger than the Coulomb repulsive forces acting among protons at distances on the order of the nuclear radius ($R \approx 1.25 \times 10^{-13} A^{1/3}$ cm) in a stable nucleus. These forces are such that the ratio of the atomic mass A (the number of neutrons plus protons) to the atomic number Z (the number of protons) increases with Z; in other words, the stable nuclides become increasingly *neutron-rich* with increasing Z, as illustrated in Fig. 1.1. The various nuclear species are referred to as *nuclides*, and nuclides with the same atomic number are referred to as *isotopes* of the *element* corresponding to Z. We use the notation ${}^{A}X_{Z}$ (e.g., ${}^{235}U_{92}$) to identify nuclides.

Binding Energy

The actual mass of an atomic nucleus is not the sum of the masses (m_p) of the Z protons and the masses (m_n) of $A - Z$ neutrons of which it is composed. The stable nuclides have a mass defect

$$\Delta = [Zm_p + (A - Z)m_n] - {}^{A}m_z \tag{1.1}$$

This mass defect is conceptually thought of as having been converted to energy ($E = \Delta c^2$) at the time that the nucleus was formed, putting the nucleus into a negative energy state. The amount of externally supplied energy that would have

Nuclear Reactor Physics. Weston M. Stacey

ISBN: 978-3-527-40679-1

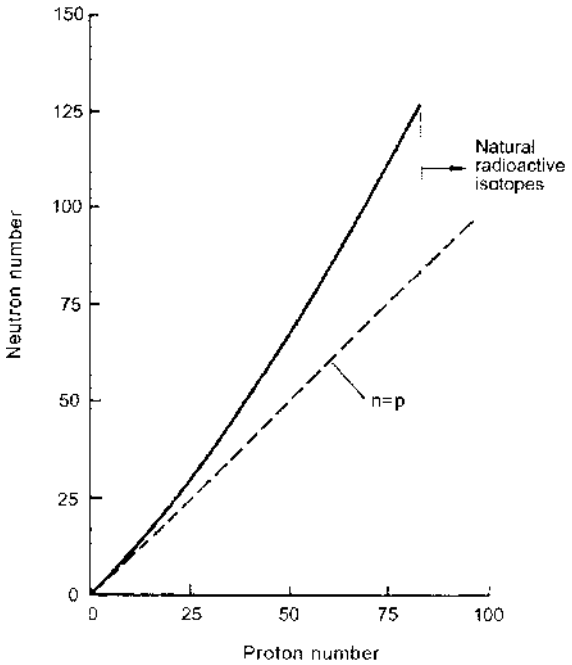

Fig. 1.1 Nuclear stability curve. (From Ref. 1; used with permission of McGraw-Hill.)

to be converted to mass in disassembling a nucleus into its separate nucleons is known as the *binding energy* of the nucleus, $\mathrm{BE} = \Delta c^2$. The binding energy per nucleon (BE/A) is shown in Fig. 1.2.

Any process that results in nuclides being converted to other nuclides with more binding energy per nucleon will result in the conversion of mass into energy. The combination of low A nuclides to form higher A nuclides with a higher BE/A value is the basis for the *fusion* process for the release of nuclear energy. The splitting of very high A nuclides to form intermediate-A nuclides with a higher BE/A value is the basis of the *fission* process for the release of nuclear energy.

Threshold External Energy for Fission

The probability of any nuclide undergoing fission (reconfiguring its A nucleons into two nuclides of lower A) can become quite large if a sufficient amount of external energy is supplied to excite the nucleus. The minimum, or *threshold*, amount of such *excitation energy* required to cause fission with high probability depends on the nuclear structure and is quite large for nuclides with $Z < 90$. For nuclides with $Z > 90$, the threshold energy is about 4 to 6 MeV for even-A nuclides, and generally is much lower for odd-A nuclides. Certain of the heavier nuclides (e.g., $^{240}\mathrm{Pu}_{94}$ and $^{252}\mathrm{Cf}_{98}$) exhibit significant spontaneous fission even in the absence of any externally supplied excitation energy.

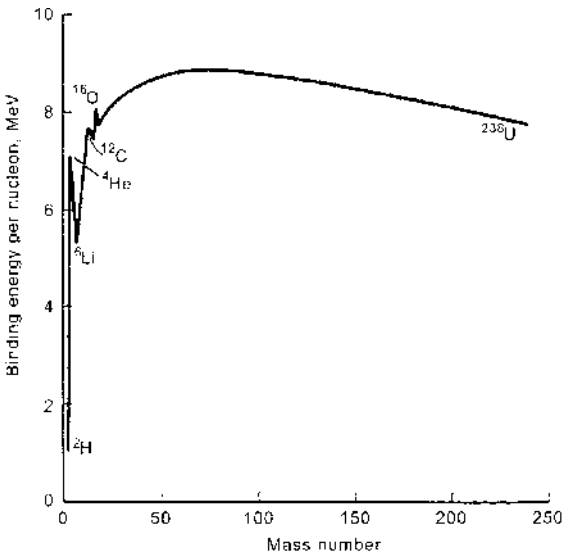

Fig. 1.2 Binding energy per nucleon. (From Ref. 1; used with permission of McGraw-Hill.)

Neutron-Induced Fission

When a neutron is absorbed into a heavy nucleus (A, Z) to form a *compound nucleus* $(A + 1, Z)$, the BE/A value is lower for the compound nucleus than for the original nucleus. For some nuclides (e.g., $^{233}U_{92}$, $^{235}U_{92}$, $^{239}Pu_{94}$, $^{241}Pu_{94}$), this reduction in BE/A value is sufficient that the compound nucleus will undergo fission, with high probability, even if the neutron has very low energy. Such nuclides are referred to as *fissile*; that is, they can be caused to undergo fission by the absorption of a low-energy neutron. If the neutron had kinetic energy prior to being absorbed into a nucleus, this energy is transformed into additional excitation energy of the compound nucleus. All nuclides with $Z > 90$ will undergo fission with high probability when a neutron with kinetic energy in excess of about 1 MeV is absorbed. Nuclides such as $^{232}Th_{90}$, $^{238}U_{92}$, and $^{240}Pu_{94}$ will undergo fission with neutrons with energy of about 1 MeV or higher, with high probability.

Neutron Fission Cross Sections

The probability of a nuclear reaction, in this case fission, taking place can be expressed in terms of a quantity σ which expresses the probable reaction rate for n neutrons traveling with speed v a distance dx in a material with N nuclides per unit volume:

$$\sigma \equiv \frac{\text{reaction rate}}{n\text{v}N\,dx} \tag{1.2}$$

The units of σ are area, which gives rise to the concept of σ as a cross-sectional area presented to the neutron by the nucleus, for a particular reaction process, and

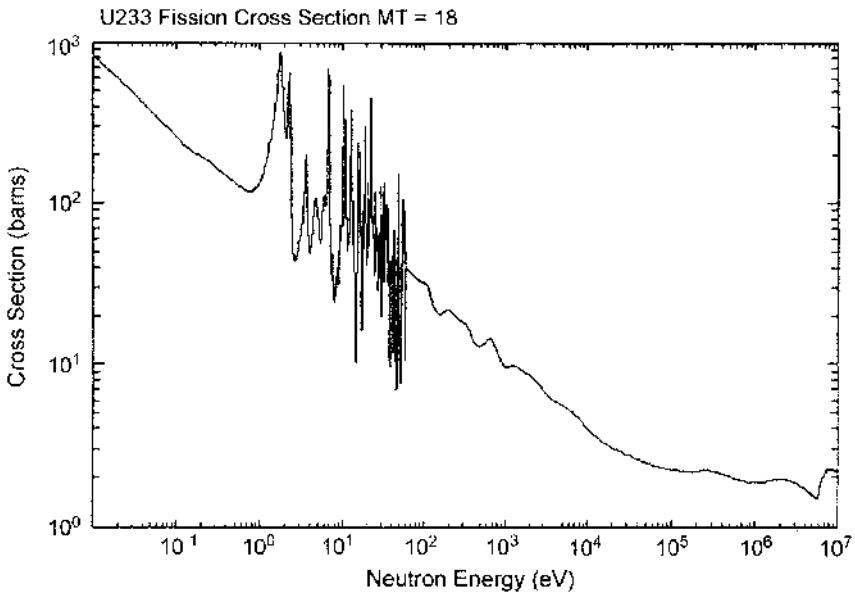

Fig. 1.3 Fission cross sections for $^{233}U_{92}$. (From *http://www.nndc.bnl.gov/*.)

to the designation of σ as a *cross section*. Cross sections are usually on the order of 10^{-24} cm^2, and this unit is referred to as a *barn*, for historical reasons.

The fission cross section, σ_f, is a measure of the probability that a neutron and a nucleus interact to form a compound nucleus which then undergoes fission. The probability that a compound nucleus will be formed is greatly enhanced if the relative energy of the neutron and the original nucleus, plus the reduction in the nuclear binding energy, corresponds to the difference in energy of the ground state and an excited state of the compound nucleus, so that the energetics are just right for formation of a compound nucleus in an excited state. The first excited states of the compound nuclei resulting from neutron absorption by odd-A fissile nuclides are generally lower lying (nearer to the ground state) than are the first excited states of the compound nuclei resulting from neutron absorption by the heavy even-A nuclides, which accounts for the odd-A nuclides having much larger absorption and fission cross sections for low-energy neutrons than do the even-A nuclides.

Fission cross sections for some of the principal fissile nuclides of interest for nuclear reactors are shown in Figs. 1.3 to 1.5. The resonance structure corresponds to the formation of excited states of the compound nuclei, the lowest lying of which are at less than 1 eV. The nature of the resonance cross section can be shown to give rise to a $1/E^{1/2}$ or $1/\upsilon$ dependence of the cross section at off-resonance neutron energies below and above the resonance range, as is evident in these figures. The fission cross sections are largest in the thermal energy region $E < \sim 1$ eV. The thermal fission cross section for $^{239}Pu_{94}$ is larger than that of $^{235}U_{92}$ or $^{233}U_{92}$.

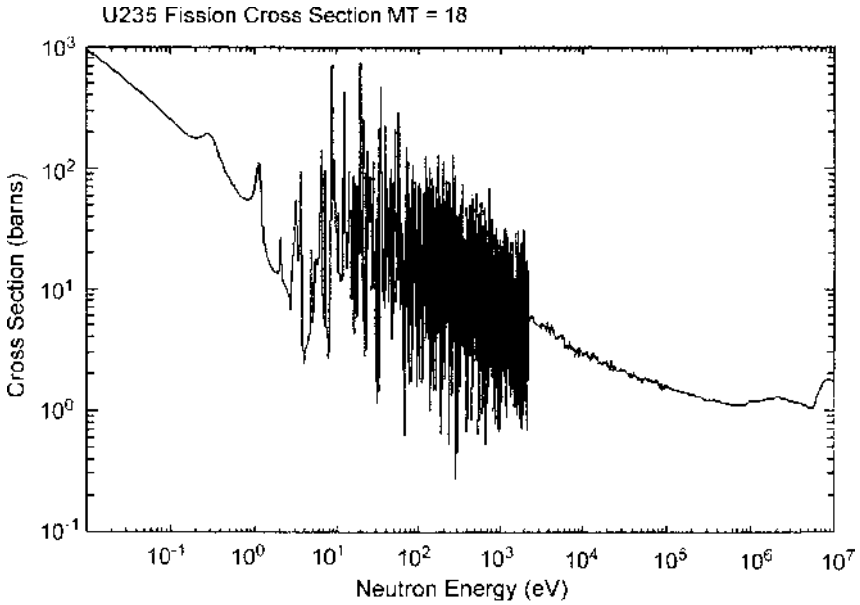

Fig. 1.4 Fission cross sections for $^{235}U_{92}$. (From *http://www.nndc.bnl.gov/*.)

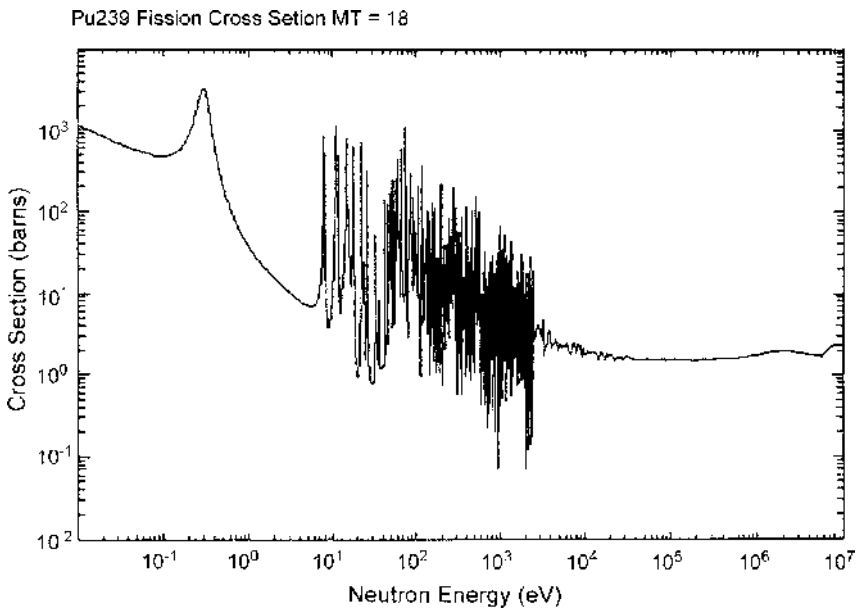

Fig. 1.5 Fission cross sections for $^{239}Pu_{94}$. (From *http://www.nndc.bnl.gov/*.)

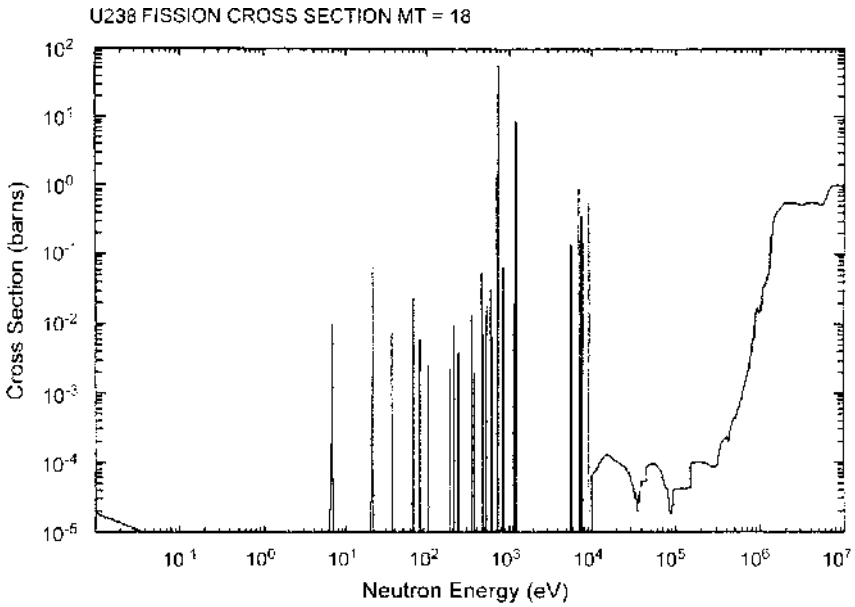

Fig. 1.6 Fission cross sections for $^{238}U_{92}$. (From *http://www.nndc.bnl.gov/*.)

Fission cross sections for $^{238}U_{92}$ and $^{240}Pu_{94}$ are shown in Figs. 1.6 and 1.7. Except for resonances, the fission cross section is insignificant below about 1 MeV, above which it is about 1 barn. The fission cross sections for these and other even-A heavy mass nuclides are compared in Fig. 1.8, without the resonance structure.

Products of the Fission Reaction

A wide range of nuclides are formed by the fission of heavy mass nuclides, but the distribution of these fission fragments is sharply peaked in the mass ranges $90 < A < 100$ and $135 < A < 145$, as shown in Fig. 1.9. With reference to the curvature of the trajectory of the stable isotopes on the n versus p plot of Fig. 1.1, most of these fission fragments are above the stable isotopes (i.e., are neutron rich) and will decay, usually by β-decay (electron emission), which transmutes the fission fragment nuclide (A, Z) to $(A, Z + 1)$, or sometimes by neutron emission, which transmutes the fission fragment nuclide (A, Z) to $(A - 1, Z)$, in both instances toward the range of stable isotopes. Sometimes several decay steps are necessary to reach a stable isotope.

Usually either two or three neutrons will be emitted promptly in the fission event, and there is a probability of one or more neutrons being emitted subsequently upon the decay of neutron-rich fission fragments over the next second or so. The number of neutrons, on average, which are emitted in the fission process, ν, depends on the fissioning nuclide and on the energy of the neutron inducing fission, as shown in Fig. 1.10.

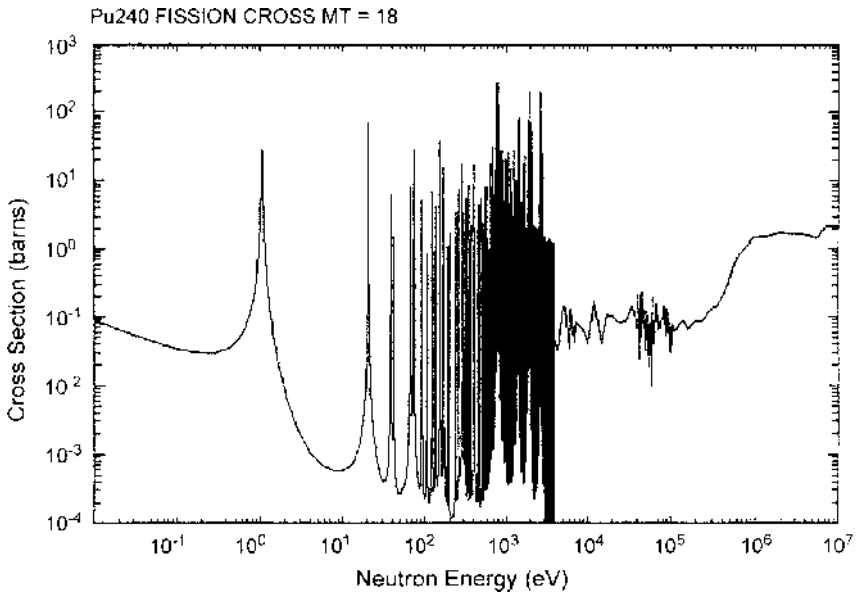

Fig. 1.7 Fission cross sections for $^{240}Pu_{94}$. (From *http://www.nndc.bnl.gov/*.)

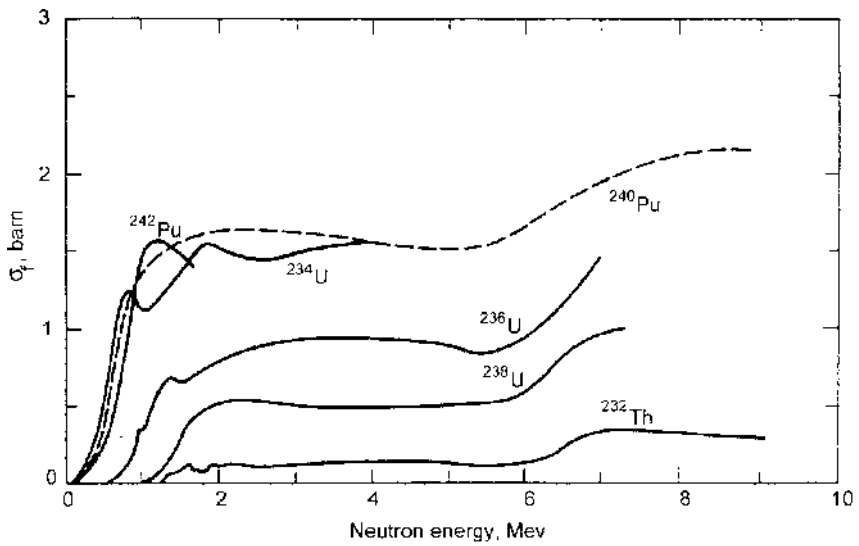

Fig. 1.8 Fission cross sections for principal nonfissile heavy mass nuclides. (From Ref. 15; used with permission of Argonne National Laboratory.)

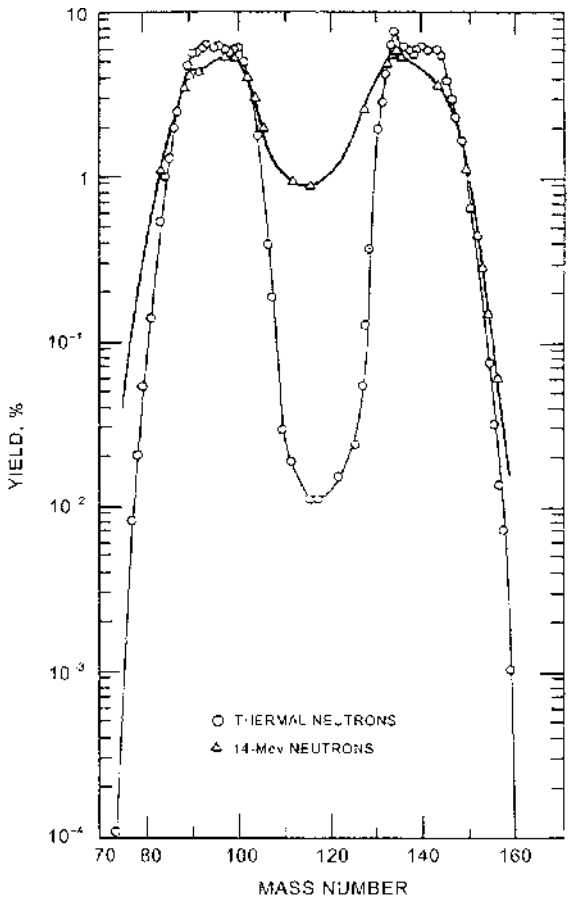

Fig. 1.9 Yield versus mass number for $^{235}U_{92}$ fission. (From Ref. 15.)

Energy Release

The majority of the nuclear energy created by the conversion of mass to energy in the fission event (207 MeV for $^{233}U_{92}$) is in the form of the kinetic energy (168 MeV) of the recoiling fission fragments. The range of these massive, highly charged particles in the fuel element is a fraction of a millimeter, so that the recoil energy is effectively deposited as heat at the point of fission. Another 5 MeV is in the form of kinetic energy of prompt neutrons released in the fission event, distributed in energy as shown in Fig. 1.11, with a most likely energy of 0.7 MeV (for $^{235}U_{92}$). This energy is deposited in the surrounding material within 10 to 100 cm as the neutron diffuses, slows down by scattering collisions with nuclei, and is finally absorbed. A fraction of these neutron absorption events result in neutron capture followed by gamma emission, producing on average about 7 MeV in the form of energetic capture gammas per fission. This secondary capture gamma en-

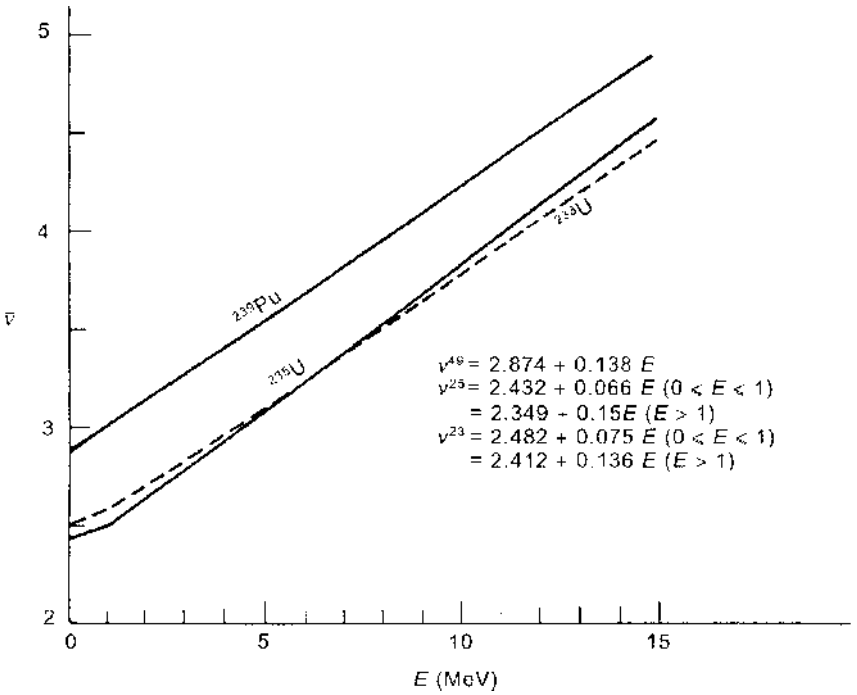

Fig. 1.10 Average number of neutrons emitted per fission. (From Ref. 12; used with permission of Wiley.)

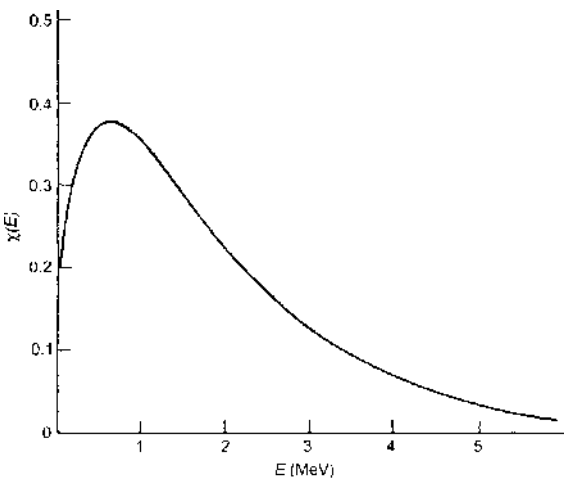

Fig. 1.11 Fission spectrum for thermal neutron-induced fission in $^{235}U_{92}$. (From Ref. 12; used with permission of Wiley.)

Table 1.1 $^{235}U_{92}$ Fission Energy Release

Form	Energy (MeV)	Range
Kinetic energy fission products	168	< mm
Kinetic energy prompt gammas	7	10–100 cm
Kinetic energy prompt neutrons	5	10–100 cm
Kinetic energy capture gammas	7	10–100 cm
Decay of fission products		
Kinetic energy electrons	8	∼mm
Kinetic energy neutrinos	12	∞

ergy is transferred as heat to the surrounding material over a range of 10 to 100 cm by gamma interactions.

There is also on average about 7 MeV of fission energy directly released as gamma rays in the fission event, which is deposited as heat within the surrounding 10 to 100 cm. The remaining 20 MeV of fission energy is in the form of kinetic energy of electrons (8 MeV) and neutrinos (12 MeV) from the decay of the fission fragments. The electron energy is deposited, essentially in the fuel element, within about 1 mm of the fission fragment, but since neutrinos rarely interact with matter, the neutrino energy is lost. Although the kinetic energy of the neutrons emitted by the decay of fission products is almost as great as that of the prompt fission neutrons, there are so few delayed neutrons from fission product decay that their contribution to the fission energy distribution is negligible. This fission energy distribution for $^{235}U_{92}$ is summarized in Table 1.1. The recoverable energy released from fission by thermal and fission spectrum neutrons is given in Table 1.2.

Table 1.2 Recoverable Energy from Fission

Isotope	Thermal Neutron	Fission Neutron
^{233}U	190.0	–
^{235}U	192.9	–
^{239}Pu	198.5	–
^{241}Pu	200.3	–
^{232}Th	–	184.2
^{234}U	–	188.9
^{236}U	–	191.4
^{238}U	–	193.9
^{237}Np	–	193.6
^{238}Pu	–	196.9
^{240}Pu	–	196.9
^{242}Pu	–	200.0

Source: Data from Ref. 12; used with permission of Wiley.

Thus, in total, about 200 MeV per fission of heat energy is produced. One Watt of heat energy then corresponds to the fission of 3.1×10^{10} nuclei per second. Since 1 g of any fissile nuclide contains about 2.5×10^{21} nuclei, the fissioning of 1 g of fissile material produces about 1 megawatt-day (MWd) of heat energy. Because some fissile nuclei will also be transmuted by neutron capture, the amount of fissile material destroyed is greater than the amount fissioned.

1.2
Neutron Capture

Radiative Capture

When a neutron is absorbed by a nucleus to form a compound nucleus, a number of reactions are possible, in addition to fission, in the heavy nuclides. We have already mentioned *radiative capture*, in which the compound nucleus decays by the emission of a gamma ray, and we now consider this process in more detail. An energy-level diagram for the compound nucleus formation and decay associated with the prominent $^{238}U_{92}$ resonance for incident neutron energies of about 6.67 eV is shown in Fig. 1.12. The energy in the center-of-mass (CM) system of an incident neutron with energy E_L in the lab system is $E_c = [A/(1 + A)]E_L$. The reduction in binding energy due to the absorbed neutron is ΔE_B. If $E_c + \Delta E_B$ is close to an excited energy level of the compound nucleus, the probability for com-

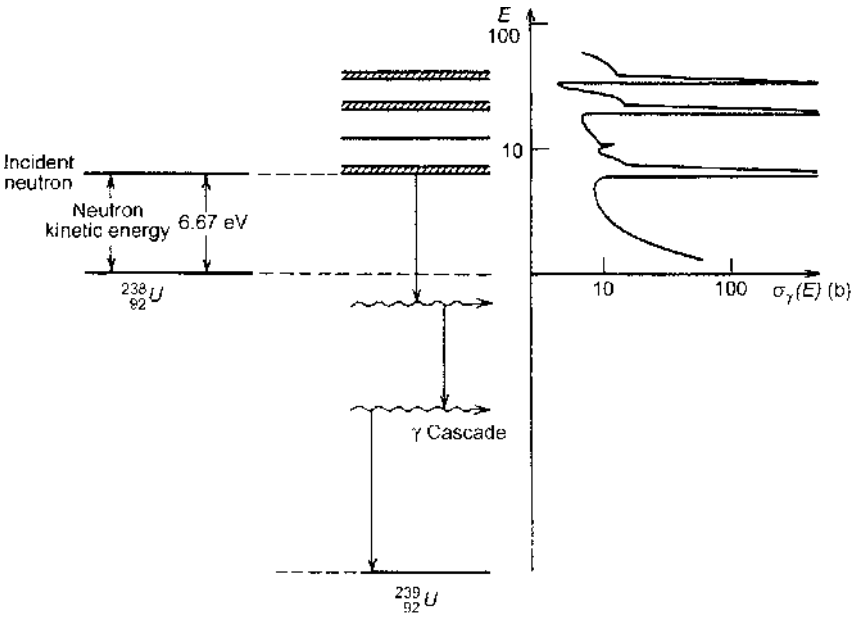

Fig. 1.12 Energy-level diagram for compound nucleus formation. (From Ref. 12; used with permission of Wiley.)

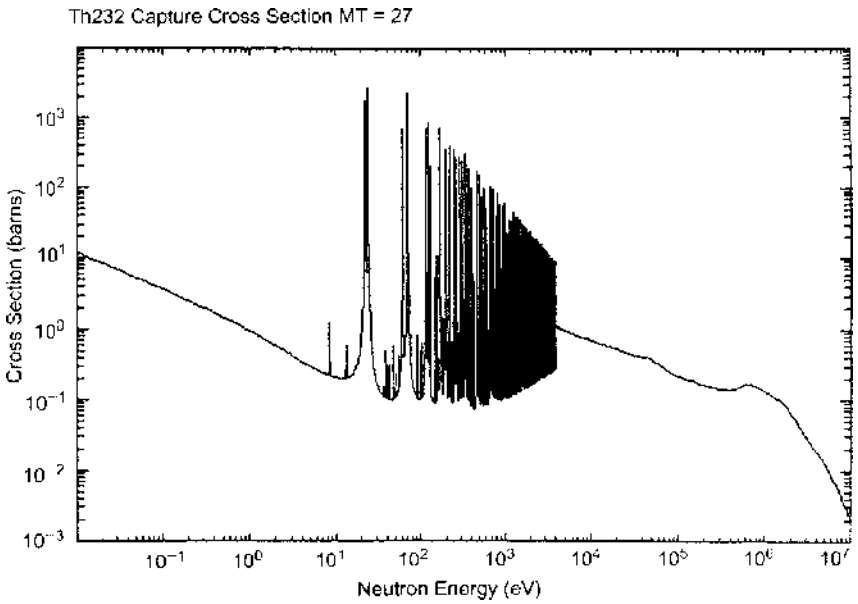

Fig. 1.13 Radiative capture cross section for $^{232}Th_{90}$. (From *http://www.nndc.bnl.gov/*.)

pound nucleus formation is greatly enhanced. The excited compound nucleus will generally decay by emission of one or more gamma rays, the combined energy of which is equal to the difference in the excited- and ground-state energy levels of the compound nucleus.

Radiative capture cross sections, denoted σ_γ, for some nuclei of interest for nuclear reactors are shown in Figs. 1.13 to 1.21. The resonance nature of the cross sections over certain ranges correspond to the discrete excited states of the compound nucleus that is formed upon neutron capture. These excited states correspond to neutron energies in the range of a fraction of an eV to 10^3 eV for the fissile nuclides, generally correspond to neutron energies of 10 to 10^4 eV for even-A heavy mass nuclides (with the notable exception of thermal $^{240}Pu_{94}$ resonance), and correspond to much higher neutron energies for the lower mass nuclides. The $1/v$ "off-resonance" cross-section dependence is apparent.

The Breit–Wigner single-level resonance formula for the neutron capture cross section is

$$\sigma_\gamma(E_c) = \sigma_0 \frac{\Gamma_\gamma}{\Gamma} \left(\frac{E_0}{E_c}\right)^{1/2} \frac{1}{1+y^2}, \qquad y = \frac{2}{\Gamma}(E_c - E_0) \tag{1.3}$$

where E_0 is the energy (in the CM) system at which the resonance peak occurs (i.e., $E_c + \Delta E_B$ matches the energy of an excited state of the compound nucleus), Γ the full width at half-maximum of the resonance, σ_0 the maximum value of the total cross section (at E_0), and Γ_γ the radiative capture width (Γ_γ/Γ is the probability that the compound nucleus, once formed, will decay by gamma emission). The

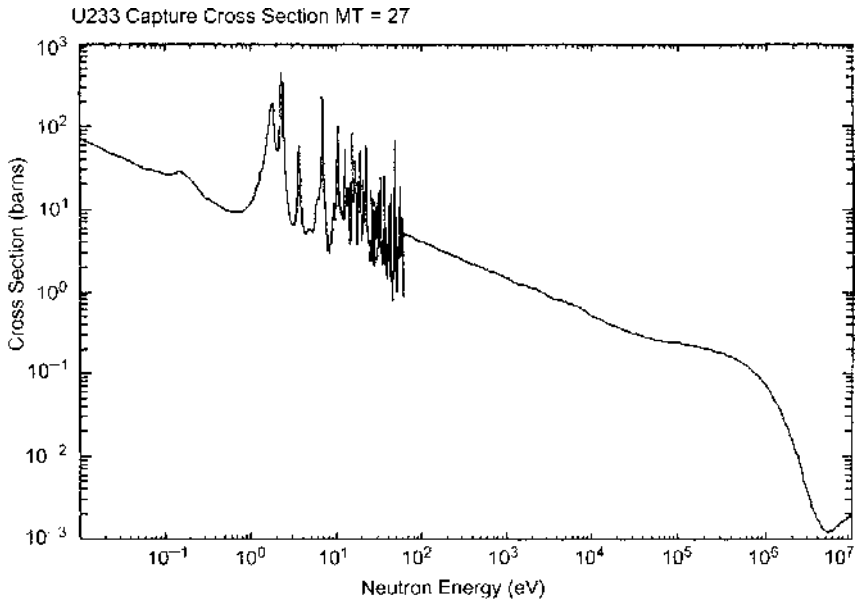

Fig. 1.14 Radiative capture cross section for $^{233}U_{92}$. (From *http://www.nndc.bnl.gov/*.)

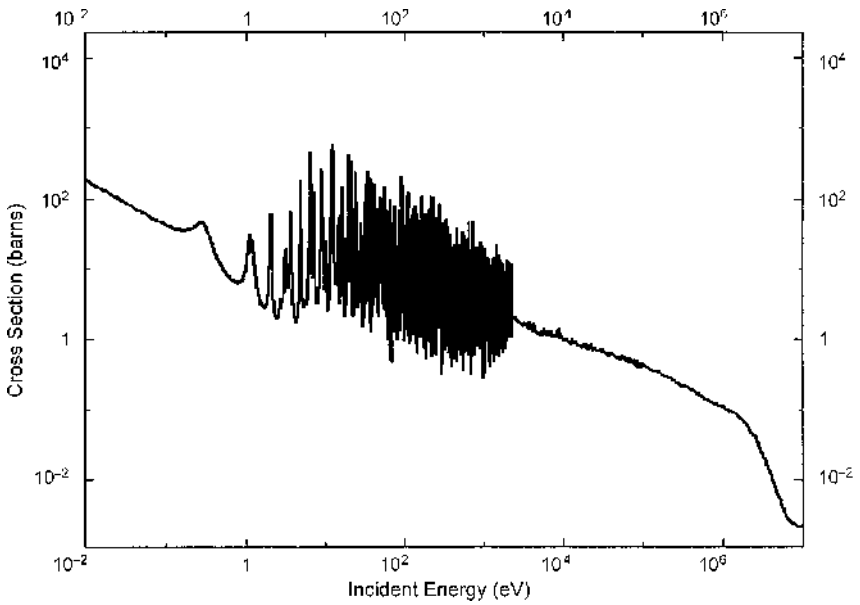

Fig. 1.15 Radiative capture cross section for $^{235}U_{92}$. (From *http://www.nndc.bnl.gov/*.)

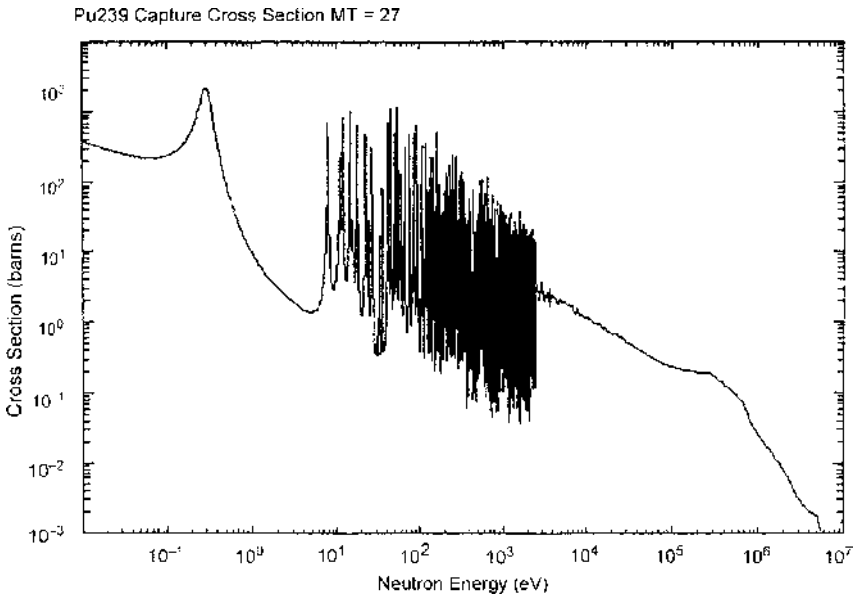

Fig. 1.16 Radiative capture cross section for $^{239}Pu_{94}$. (From *http://www.nndc.bnl.gov/*.)

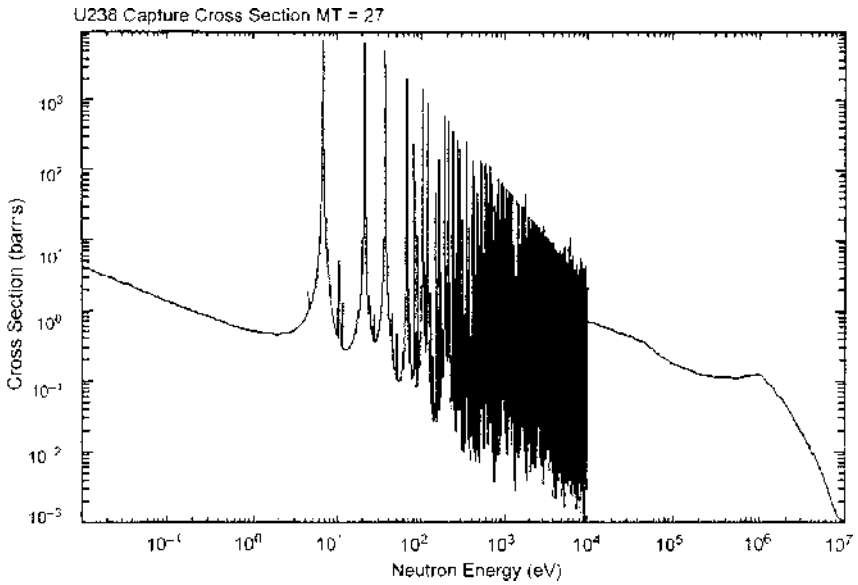

Fig. 1.17 Radiative capture cross section for $^{238}U_{92}$. (From *http://www.nndc.bnl.gov/*.)

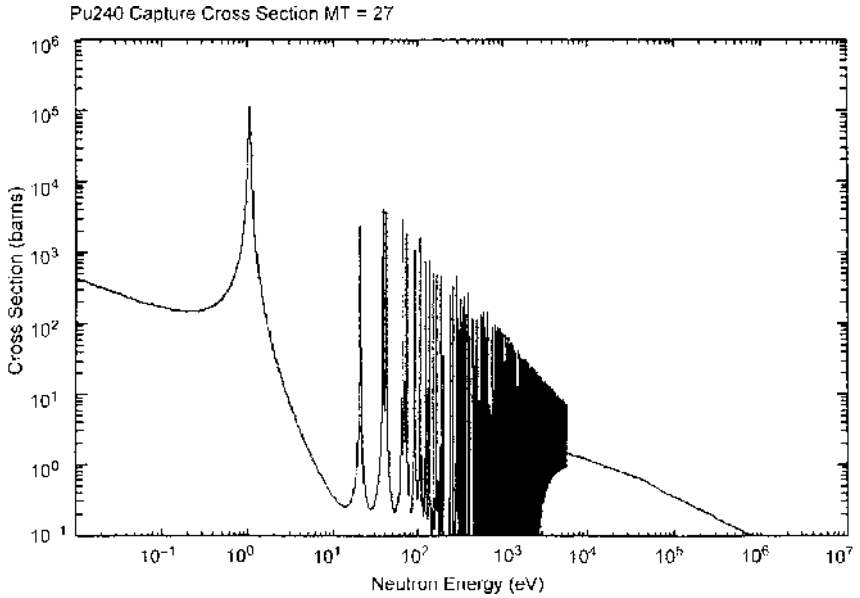

Fig. 1.18 Radiative capture cross section for $^{240}Pu_{94}$. (From *http://www.nndc.bnl.gov/*.)

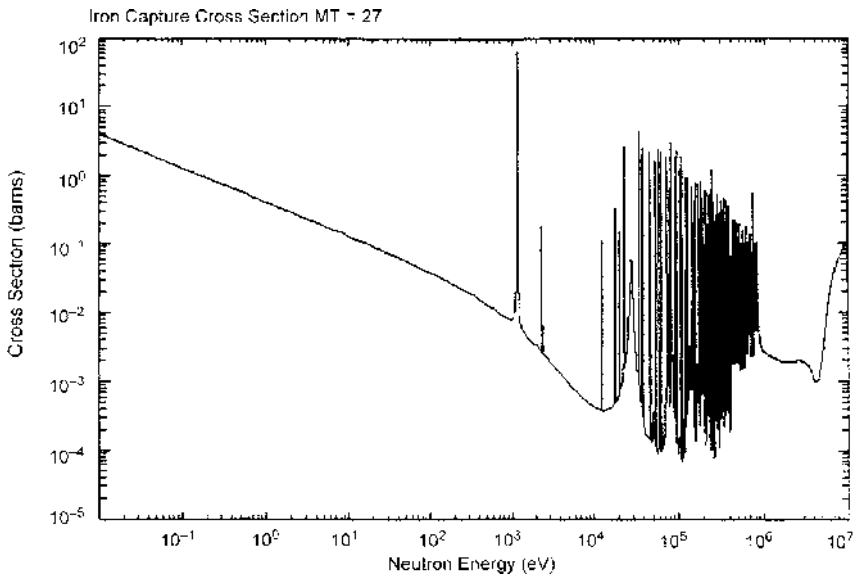

Fig. 1.19 Radiative capture cross section for $^{56}Fe_{26}$. (From *http://www.nndc.bnl.gov/*.)

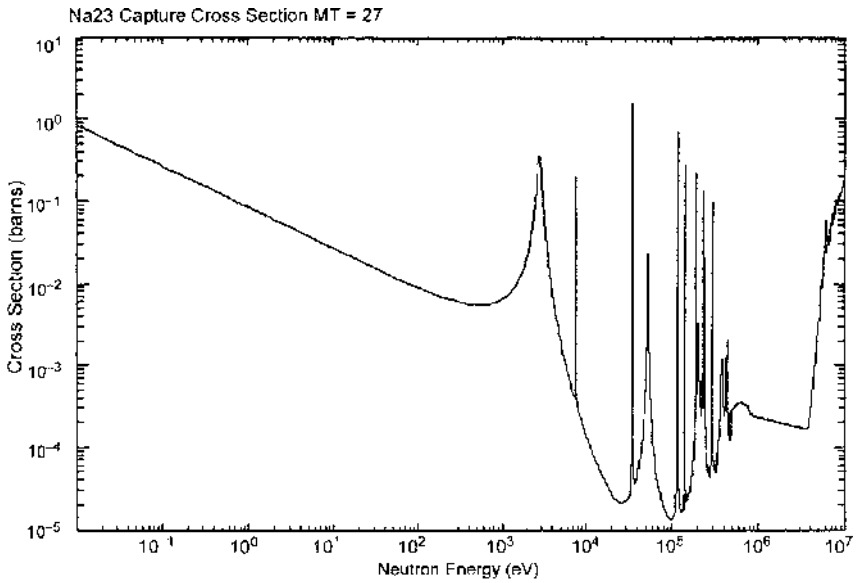

Fig. 1.20 Radiative capture cross section for $^{23}Na_{11}$. (From *http://www.nndc.bnl.gov/*.)

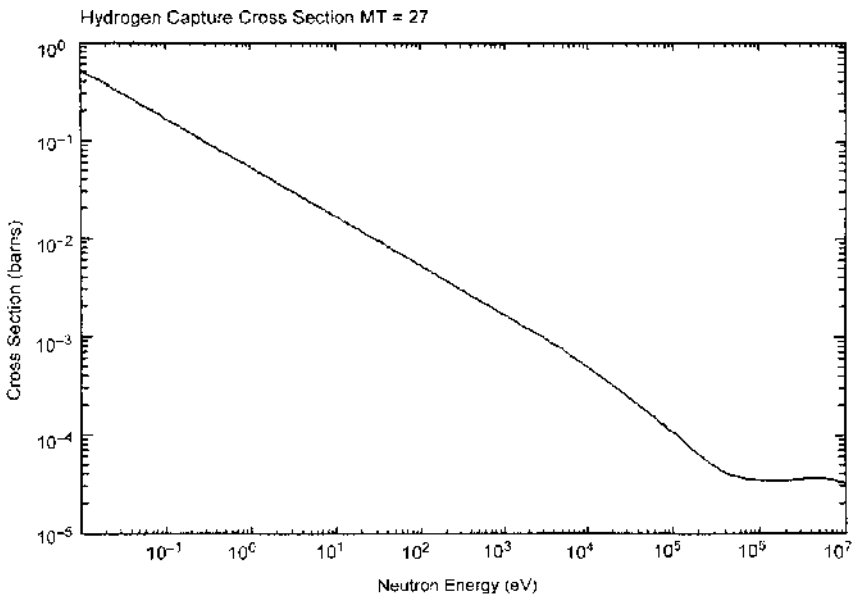

Fig. 1.21 Radiative capture cross section for $^{1}H_{1}$. (From *http://www.nndc.bnl.gov/*.)

fission resonance cross section can be represented by a similar expression with the fission width Γ_f, defined such that Γ_f/Γ is the probability that the compound nucleus, once formed, will decay by fission.

Equation (1.3) represents the cross section describing the interaction of a neutron and nucleus with relative (CM) energy E_c. However, the nuclei in a material are distributed in energy (approximately a Maxwellian distribution characterized by the temperature of the material). What is needed is a cross section averaged over the motion of the nuclei:

$$\bar{\sigma}(E,T) = \frac{1}{\upsilon(E)} \int dE' \, |\mathbf{v}(E) - \mathbf{v}(E')| \, \sigma(E_c) \, f_{\max}(E', T) \tag{1.4}$$

where E and E' are the neutron and nuclei energies, respectively, in the lab system, and $f_{\max}(E')$ is the Maxwellian energy distribution:

$$f_{\max}(E') = \frac{2\pi}{(\pi kT)^{3/2}} \sqrt{E'} e^{-E'/kT} \tag{1.5}$$

Using Eqs. (1.3) and (1.5), Eq. (1.4) becomes

$$\bar{\sigma}_\gamma(E,T) = \frac{\sigma_0 \Gamma_\gamma}{\Gamma} \left(\frac{E_0}{E} \right)^{1/2} \Psi(\xi, x) \tag{1.6}$$

where

$$x = \frac{2}{\Gamma}(E - E_0), \qquad \xi = \frac{\Gamma}{(4E_0 kT/A)^{1/2}} \tag{1.7}$$

A is the atomic mass (amu) of the nuclei, and

$$\Psi(\xi, x) = \frac{\xi}{2\sqrt{\pi}} \int_{-\infty}^{\infty} e^{-(1/4)(x-y)^2 \xi^2} \frac{dy}{1 + y^2} \tag{1.8}$$

Neutron Emission

When the compound nucleus formed by neutron capture decays by the emission of one neutron, leaving the nucleus in an excited state which subsequently undergoes further decays, the event is referred to as *inelastic scattering* and the cross section is denoted σ_{in}. Since the nucleus is left in an excited state, the energy of the emitted neutron can be considerably less than the energy of the incident neutron. If the compound nucleus decays by the emission of two or more neutrons, the events are referred to as $n - 2n$, $n - 3n$, and so on, events, and the cross sections are denoted $\sigma_{n,2n}$, $\sigma_{n,3n}$, on so on. Increasingly higher incident neutron energies are required to provide enough excitation energy for single, double, triple, and so on, neutron emission. Inelastic scattering is the most important of these events in nuclear reactors, but it is most important for neutrons 1 MeV and higher in energy.

1.3 Neutron Elastic Scattering

Elastic scattering may take place via compound nucleus formation followed by the emission of a neutron that returns the compound nucleus to the ground state of the original nucleus. In such a resonance elastic scattering event the kinetic energy of the original neutron–nuclear system is conserved. The neutron and the nucleus may also interact without neutron absorption and the formation of a compound nucleus, which is referred to as *potential scattering*. Although quantum mechanical (*s*-wave) in nature, the latter event may be visualized and treated as a classical hard-sphere scattering event, away from resonance energies. Near resonance energies, there is quantum mechanical interference between the potential and resonance scattering, which is constructive just above and destructive just below the resonance energy.

The single-level Breit–Wigner form of the scattering cross section, modified to include potential and interference scattering, is

$$\sigma_s(E_c) = \sigma_0 \frac{\Gamma_n}{\Gamma} \left(\frac{E_0}{E_c}\right)^{1/2} \frac{1}{1+y^2} + \frac{\sigma_0 2R}{\lambda_0} \frac{y}{1+y^2} + 4\pi R^2 \tag{1.9}$$

where (Γ_n/Γ) is the probability that, once formed, the compound nucleus decays to the ground state of the original nucleus by neutron emission, $R \simeq 1.25 \times 10^{-13} A^{1/3}$ centimeters is the nuclear radius, and λ_0 is the reduced neutron wavelength.

Averaging over a Maxwellian distribution of nuclear motion yields the scattering cross section for neutron lab energy E and material temperature T:

$$\bar{\sigma}_s(E,T) = \sigma_0 \frac{\Gamma_n}{\Gamma} \psi(\xi, x) + \frac{\sigma_0 R}{\lambda_0} \chi(\xi, x) + 4\pi R^2 \tag{1.10}$$

where

$$\chi(\xi, x) = \frac{\xi}{\sqrt{\pi}} \int_{-\infty}^{\infty} \frac{y e^{-(1/4)(x-y)^2 \xi^2}}{1+y^2} dy \tag{1.11}$$

The elastic scattering cross sections for a number of nuclides of interest in nuclear reactors are shown in Figs. 1.22 to 1.26. In general, the elastic scattering cross section is almost constant in energy below the neutron energies corresponding to the excited states of the compound nucleus. The destructive interference effects just below the resonance energy are very evident in Fig. 1.26.

The energy dependence of the carbon scattering cross section is extended to very low neutron energies in Fig. 1.27 to illustrate another phenomenon. At sufficiently small neutron energy, the neutron wavelength

$$\lambda_0 = \frac{h}{p} = \frac{h}{\sqrt{2mE}} = \frac{2.86 \times 10^{-9}}{\sqrt{E(\text{eV})}} \text{ cm} \tag{1.12}$$

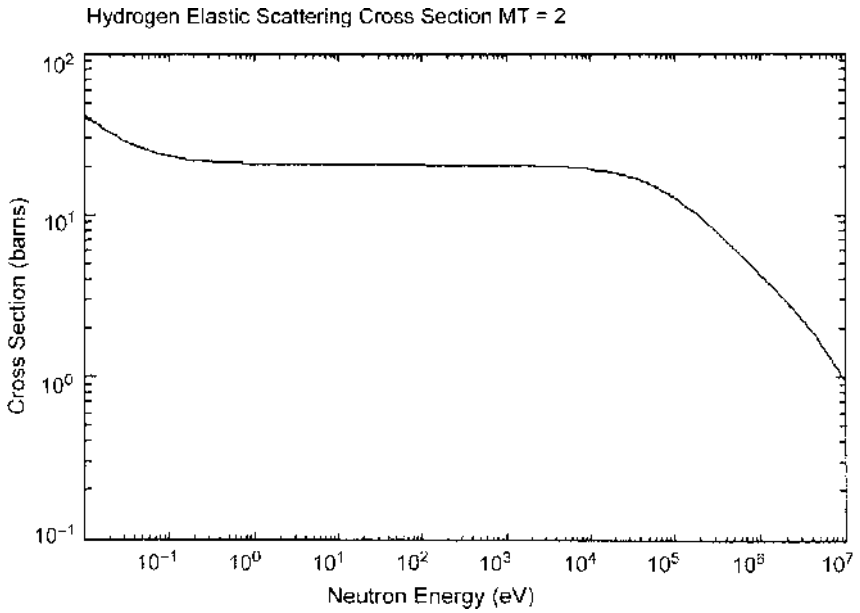

Fig. 1.22 Elastic scattering cross section for $^{1}H_{1}$. (From *http://www.nndc.bnl.gov/*.)

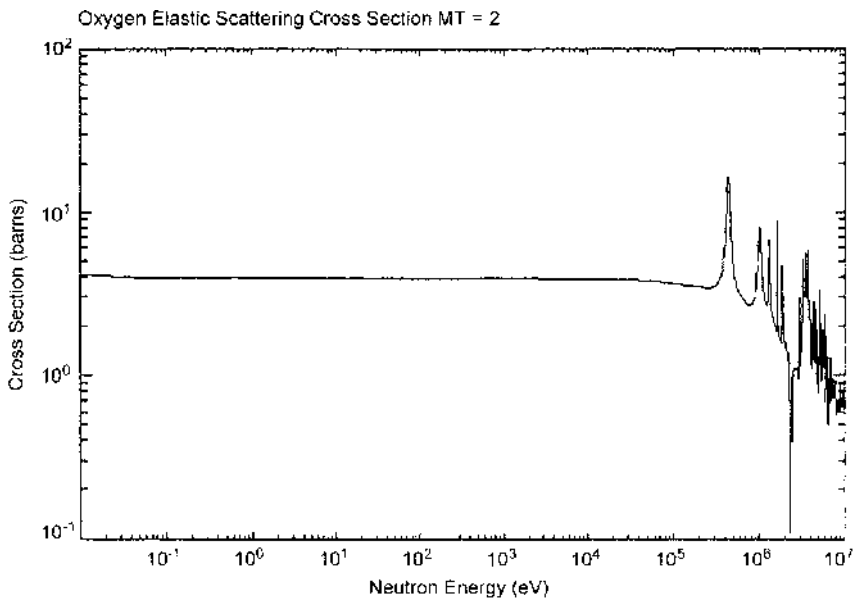

Fig. 1.23 Elastic scattering cross section for $^{16}O_{8}$. (From *http://www.nndc.bnl.gov/*.)

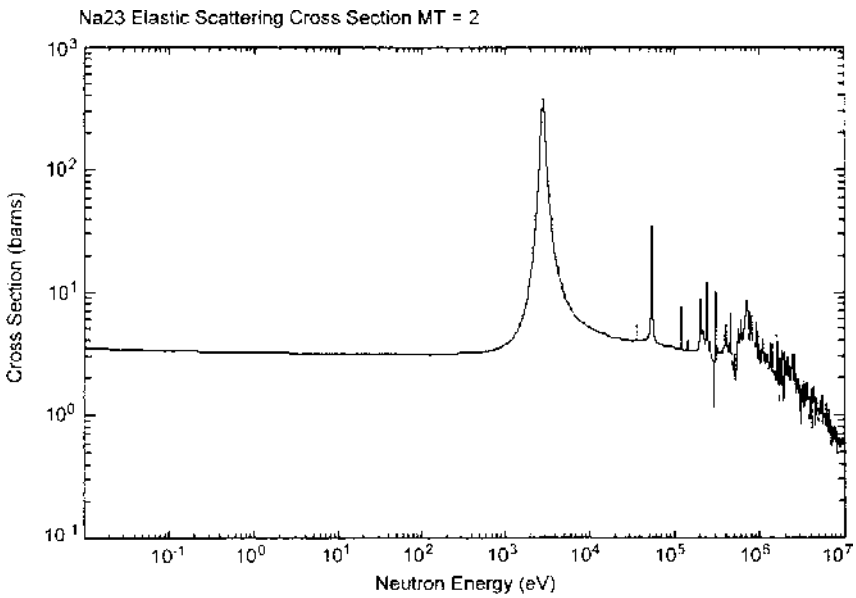

Fig. 1.24 Elastic scattering cross section for $^{23}Na_{11}$. (From *http://www.nndc.bnl.gov/*.)

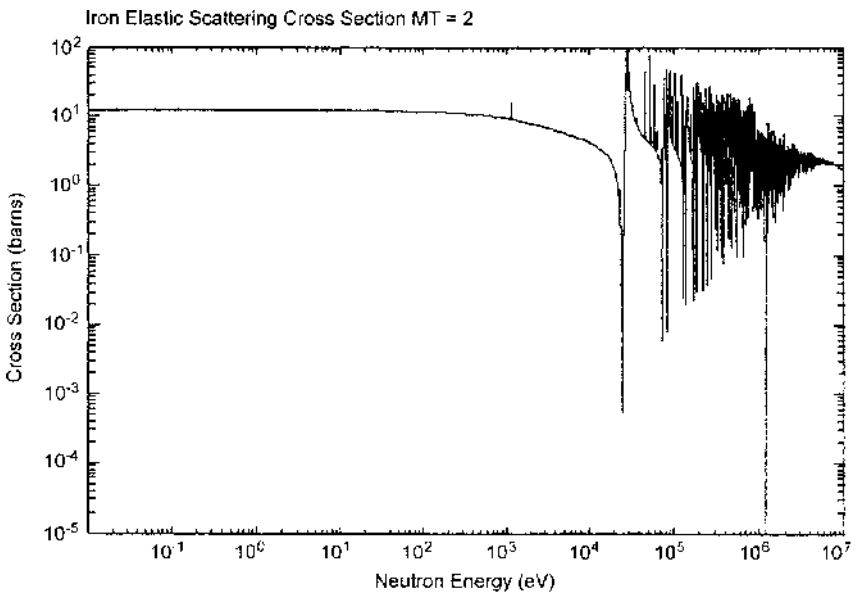

Fig. 1.25 Elastic scattering cross section for $^{56}Fe_{26}$. (From *http://www.nndc.bnl.gov/*.)

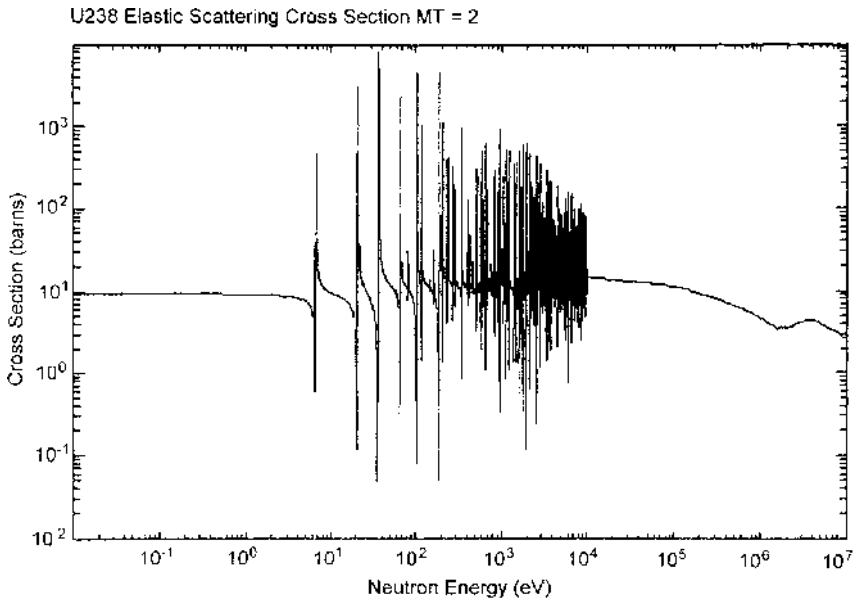

Fig. 1.26 Elastic scattering cross section for $^{238}U_{92}$. (From *http://www.nndc.bnl.gov/*.)

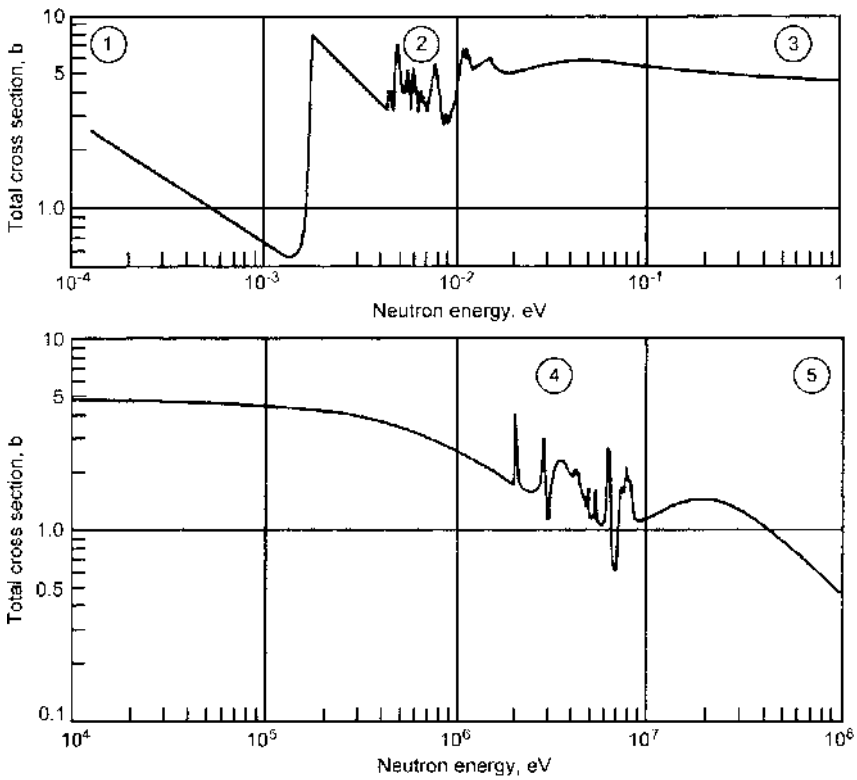

Fig. 1.27 Total scattering cross section of $^{12}C_6$. (From Ref. 12; used with permission of Wiley.)

becomes comparable to the interatomic spacing, and the neutron interacts not with a single nucleus but with an aggregate of bound nuclei. If the material has a regular structure, as graphite does, the neutron will be diffracted and the energy dependence of the cross section will reflect the neutron energies corresponding to multiples of interatomic spacing. For sufficiently small energies, diffraction becomes impossible and the cross section is once again insensitive to neutron energy.

1.4 Summary of Cross-Section Data

Low-Energy Cross Sections

The low-energy total cross sections for several nuclides of interest in nuclear reactors are plotted in Fig. 1.28. Gadolinium is sometimes used as a "burnable poison," and xenon and samarium are fission products with large thermal cross sections.

Spectrum-Averaged Cross Sections

Table 1.3 summarizes the cross-section data for a number of important nuclides in nuclear reactors. The first three columns give fission, radiative capture, and elastic scattering cross sections averaged over a Maxwellian distribution with $T = 0.0253$ eV, corresponding to a representative thermal energy spectrum. The next two columns give the infinite dilution fission and radiative capture resonance integrals, which are averages of the respective resonance cross sections over a $1/E$ spectrum typical of the resonance energy region in the limit of an infinitely dilute concentration of the resonance absorber. The final five columns give cross sections averaged over the fission spectrum.

Example 1.1: Calculation of Macroscopic Cross Section. The macroscopic cross section $\Sigma = N\sigma$, where N is the number density. The number density is related to the density ρ and atomic number A by $N = (\rho/A)N_0$, where $N_0 = 6.022 \times 10^{23}$ is Avogadro's number, the number of atoms in a mole. For a mixture of isotopes with volume fractions υ_i, the macroscopic cross section is $\Sigma = \Sigma_i \upsilon_i (\rho/A)_i N_0 \sigma_i$; for example, for a 50:50 vol % mixture of carbon and ^{238}U, the macroscopic thermal absorption cross section is $\Sigma_a = 0.5(\rho_C/A_C)N_0\sigma_{aC} + 0.5(\rho_U/A_U)N_0\sigma_{aU} = 0.5(1.60\ \text{g/cm}^3\ \text{per}\ 12\ \text{g/mol})(6.022 \times 10^{23}\ \text{atom/mol})(0.003 \times 10^{-24}\ \text{cm}^2) + 0.5(18.9\ \text{g/cm}^3\ \text{per}\ 238\ \text{g/mol})(6.022 \times 10^{23}\ \text{atom/mol})(2.4 \times 10^{-24}\ \text{cm}^2) = 0.0575\ \text{cm}^{-1}$.

1.5 Evaluated Nuclear Data Files

Published experimental and theoretical results on neutron–nuclear reactions are collected by several collaborating nuclear data agencies worldwide. Perhaps the

Table 1.3 Spectrum-Averaged Thermal, Resonance, and Fast Neutron Cross Sections (barns)

Nuclide	Thermal Cross Section			Resonance Cross Section		Fission Spectrum Cross Section				
	σ_f	σ_γ	σ_{el}	σ_f	σ_γ	σ_f	σ_γ	σ_{el}	σ_{in}	$\sigma_{n,2n}$
$^{233}U_{92}$	469	41	11.9	774	138	1.9	0.07	4.4	1.2	4×10^{-3}
$^{235}U_{92}$	507	87	15.0	278	133	1.2	0.09	4.6	1.8	12×10^{-3}
$^{239}Pu_{94}$	698	274	7.8	303	182	1.8	0.05	4.4	1.5	4×10^{-3}
$^{241}Pu_{94}$	938	326	11.1	573	180	1.6	0.12	5.2	0.9	21×10^{-3}
$^{232}Th_{90}$	–	6.5	13.7	–	84	0.08	0.09	4.6	2.9	14×10^{-3}
$^{238}U_{92}$	–	2.4	9.4	2	278	0.31	0.07	4.8	2.6	12×10^{-3}
$^{240}Pu_{94}$	0.05	264	1.5	8.9	8103	1.4	0.09	4.3	2.0	4×10^{-3}
$^{242}Pu_{94}$	–	16.8	8.3	5.6	1130	1.1	0.09	4.8	1.9	7×10^{-3}
$^{1}H_{1}$	–	0.29	20.5	–	0.15	–	4×10^{-5}	3.9	–	–
$^{2}H_{1}$	–	5×10^{-4}	3.4	–	3×10^{-4}	–	7×10^{-6}	2.5	–	–
$^{10}B_{5}$	–	443	2.1	–	0.22	–	8×10^{-5}	2.1	0.07	–
$^{12}C_{6}$	–	0.003	4.7	–	0.002	–	2×10^{-5}	2.3	0.01	–
$^{16}O_{8}$	–	2×10^{-4}	3.8	–	6×10^{-4}	–	9×10^{-5}	2.7	–	–
$^{23}Na_{11}$	–	0.47	3.0	–	0.31	–	2×10^{-4}	2.7	0.5	–
$^{56}Fe_{26}$	–	2.5	12.5	–	1.4	–	3×10^{-3}	3.0	0.7	–
$^{91}Zr_{40}$	–	1.1	10.6	–	6.9	–	0.01	5.0	0.7	–
$^{135}Xe_{54}$	–	2.7×10^{6}	3.8×10^{5}	–	7.6×10^{3}	–	0.01	4.9	1.0	–
$^{149}Sm_{62}$	–	6.0×10^{4}	373	–	3.5×10^{3}	–	0.22	4.6	2.2	–
$^{157}Gd_{64}$	–	1.9×10^{3}	819	–	761	–	0.11	4.7	2.2	11×10^{-3}

Source: Data from *http://www.nndc.bnl.gov/*.

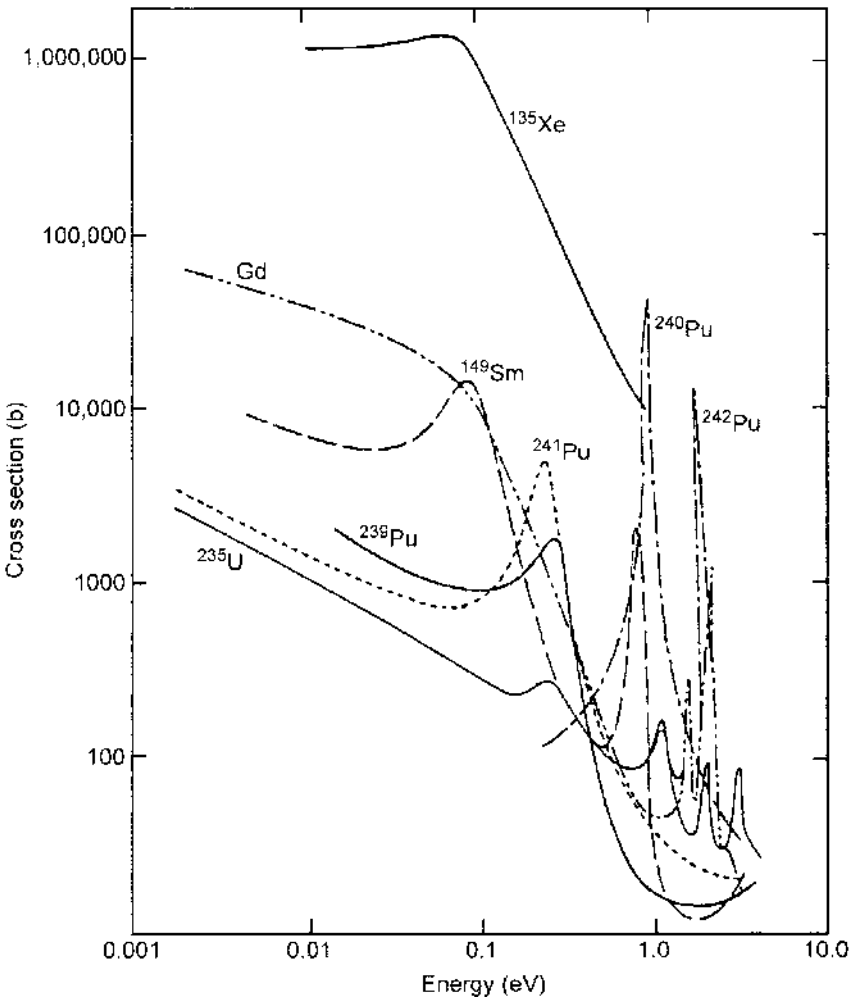

Fig. 1.28 Low-energy absorption (fission + capture) cross sections for several important nuclides. (From Ref. 12; used with permission of Wiley.)

most comprehensive computerized compilation of experimental data is the EXFOR computer library (Ref. 11). The computerized card index file CINDA (Ref. 8), which contains comprehensive information on measurements, calculations, and evaluations of neutron–nuclear data, is updated annually. The plethora of sometimes contradictory nuclear data must be evaluated before it can be used confidently in reactor physics calculations. Such evaluation consists of intercomparison of data, use of data to calculate benchmark experiments, critical assessment of statistical and systematic errors, checks for internal consistency and consistency with standard neutron cross sections, and the derivation of consistent preferred values by appropriate averaging procedures. Several large evaluated nuclear data files are maintained:

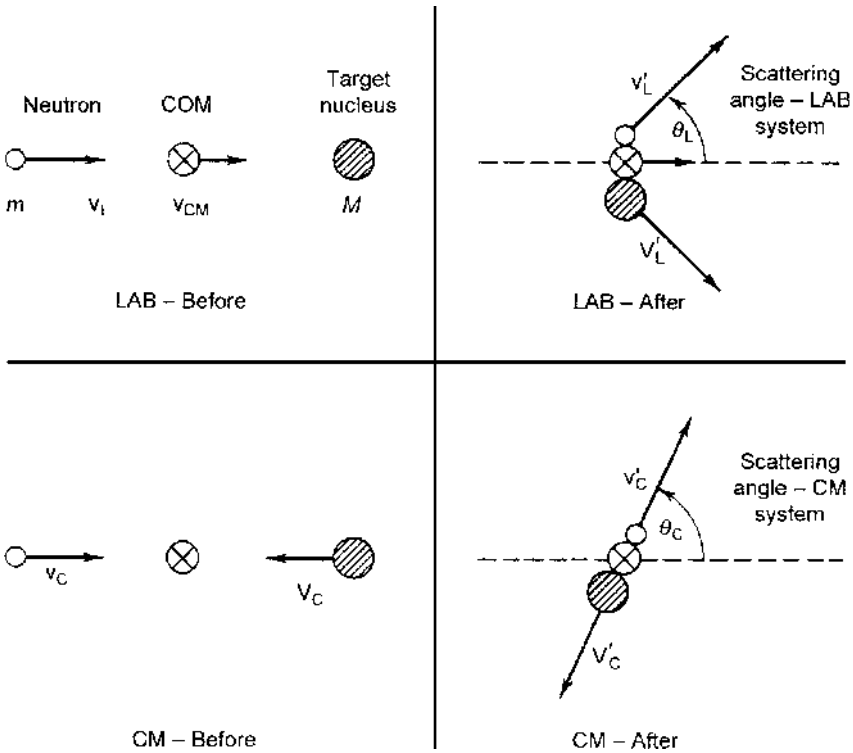

Fig. 1.29 Scattering event in lab and CM systems. (From Ref. 12; used with permission of Wiley.)

(1) United States Evaluated Nuclear Data File (ENDF/B), (2) Evaluated Nuclear Data Library of the Lawrence Livermore National Laboratory (ENDL), (3) United Kingdom Nuclear Data Library (UKNDL), (4) Japanese Evaluated Nuclear Data Library (JENDL), (5) Karlsruhe Nuclear Data File (KEDAK), (6) Russian (formerly Soviet) Evaluated Nuclear Data File (BROND), and (7) Joint Evaluated File of NEA Countries (JEF). Processing codes are used to convert these data to a form that can be used in reactor physic calculations, as discussed in subsequent chapters.

1.6
Elastic Scattering Kinematics

Consider a neutron with energy $E_L = \frac{1}{2}mv_L^2$ in the laboratory (L) system incident upon a stationary nucleus of mass M. Since only the relative masses are important in the kinematics, we set $m = 1$ and $M = A$. It is convenient to convert to the center-of-mass (CM) system, as indicated in Fig. 1.29, because the elastic scattering event is usually isotropic in the CM system.

The velocity of the CM system in the L system is

$$\mathbf{v}_{\text{cm}} = \frac{1}{1+A}(\mathbf{v}_L + A\mathbf{V}_L) = \frac{\mathbf{v}_L}{1+A} \tag{1.13}$$

and the velocities of the neutron and the nucleus in the CM system are

$$\begin{aligned} \mathbf{v}_c &= \mathbf{v}_L - \mathbf{v}_{\text{cm}} = \frac{A}{A+1}\mathbf{v}_L \\ \mathbf{V}_c &= -\mathbf{v}_{\text{cm}} = \frac{-1}{A+1}\mathbf{v}_L \end{aligned} \tag{1.14}$$

The energy of the neutron in the CM system, E_c, is related to the energy of the neutron in the lab, E_L, by

$$E_c = \frac{1}{2}\text{v}_c^2 + \frac{1}{2}AV_c^2 = \frac{A}{A+1}\frac{1}{2}\text{v}_L^2 = \frac{A}{A+1}E_L \tag{1.15}$$

Correlation of Scattering Angle and Energy Loss

From consideration of conservation of momentum and kinetic energy, it can be shown that the speeds of the neutron and the nucleus in the center-of-mass system do not change during the scattering event:

$$\begin{aligned} \text{v}_c' &= \text{v}_c = \frac{A}{A+1}\text{v}_L \\ V_c' &= V_c = \frac{-1}{A+1}\text{v}_L \end{aligned} \tag{1.16}$$

With reference to Fig. 1.30, the scattering angles in the lab and CM systems are related by

$$\tan\theta_L = \frac{\text{v}_c' \sin\theta_c}{\text{v}_{\text{cm}} + \text{v}_c' \cos\theta_c} = \frac{\sin\theta_c}{(1/A) + \cos\theta_c} \tag{1.17}$$

The law of cosines yields

$$\cos(\pi - \theta_c) = \frac{(\text{v}_c')^2 + (\text{v}_{\text{cm}})^2 - (\text{v}_L')^2}{2\text{v}_{\text{cm}}\text{v}_c'} \tag{1.18}$$

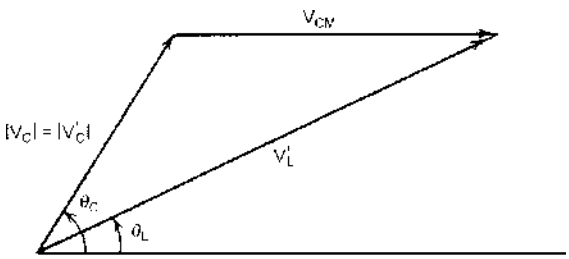

Fig. 1.30 Relation between lab and CM scattering angles. (From Ref. 12; used with permission of Wiley.)

which may be combined with Eqs. (1.13) and (1.16) to obtain a relationship between the incident and final energies of the neutron in the lab system and the scattering angle in the CM system:

$$\frac{\frac{1}{2}m(\mathrm{v}_L')^2}{\frac{1}{2}m(\mathrm{v}_L)^2} \equiv \frac{E_L'}{E_L} = \frac{A^2+1+2A\cos\theta_c}{(A+1)^2} = \frac{(1+\alpha)+(1-\alpha)\cos\theta_c}{2} \tag{1.19}$$

where $\alpha \equiv (A-1)^2/(A+1)^2$.

Average Energy Loss

Equation (1.19) states that the ratio of final to incident energies in an elastic scattering event is correlated to the scattering angle in the CM system, which in turn is correlated via Eq. (1.17) to the scattering angle in the lab system. The maximum energy loss (minimum value of E_L'/E_L) occurs for $\theta_c = \pi$ (i.e., backward scattering in the CM system), in which case $E_L' = \alpha E_L$. For hydrogen ($A = 1$), $\alpha = 0$ and all of the neutron energy can be lost in a single collision. For other nuclides, only a fraction $(1-\alpha)$ of the neutron energy can be lost in a single collision, and for heavy nuclides ($\alpha \to 1$) this fraction becomes very small.

The probability that a neutron scatters from energy E_L to within a differential band of energies dE_L' about energy E_L' is equivalent to the probability that a neutron scatters into a cone $2\pi\sin\theta_c d\theta_c$ about θ_c:

$$\sigma_s(E_L)P(E_L \to E_L')dE_L' = -\sigma_{\mathrm{cm}}(E_L,\theta_c)2\pi\sin\theta_c d\theta_c \tag{1.20}$$

where the negative sign takes into account that an increase in angle corresponds to a decrease in energy, σ_s is the elastic scattering cross section, and $\sigma_{\mathrm{cm}}(\theta_c)$ is the cross section for scattering through angle θ_c. Using Eq. (1.19) to evaluate $dE_L'/d\theta_c$, this becomes

$$P(E_L \to E_L') = \begin{cases} \dfrac{4\pi\sigma_{\mathrm{cm}}(E_L,\theta_c)}{(1-\alpha)E_L\sigma_s(E_L)}, & \alpha E_L \le E_L' \le E_L \\ 0, & \text{otherwise} \end{cases} \tag{1.21}$$

Except for very high energy neutrons scattering from heavy mass nuclides, elastic scattering in the CM is isotropic, $\sigma_{\mathrm{cm}}(\theta_c) = \sigma_s/4\pi$. In this case, Eq. (1.21) may be written

$$\begin{aligned} \sigma_s(E_L \to E_L') \equiv \sigma_s(E_L)P(E_L \to E_L') &= \frac{\sigma_s(E_L)}{(1-\alpha)E_L}, \quad \alpha E_L \le E_L' \le E_L \\ &= 0, \qquad\qquad\qquad\qquad \text{otherwise} \end{aligned} \tag{1.22}$$

The average energy loss in an elastic scattering event may be calculated from

$$\langle \Delta E_L \rangle \equiv E_L - \int_{\alpha E_L}^{E_L} dE_L' E_L' P(E_L \to E_L') = \frac{1}{2}(1-\alpha)E_L \tag{1.23}$$

Table 1.4 Number of Collisions, on Average, to Moderate a Neutron from 2 MeV to 1 eV

Moderator	ξ	Number of Collisions	$\xi\Sigma_s/\Sigma_a$
H	1.0	14	–
D	0.725	20	–
H_2O	0.920	16	71
D_2O	0.509	29	5670
He	0.425	43	83
Be	0.209	69	143
C	0.158	91	192
Na	0.084	171	1134
Fe	0.035	411	35
^{238}U	0.008	1730	0.0092

and the average logarithmic energy loss may be calculated from

$$\xi \equiv \int_{\alpha E_L}^{E_L} dE'_L \ln\left(\frac{E_L}{E'_L}\right) P(E_L \to E'_L)$$
$$= 1 + \frac{\alpha}{1-\alpha}\ln\alpha = 1 - \frac{(A-1)^2}{2A}\ln\left(\frac{A+1}{A-1}\right) \tag{1.24}$$

The number of collisions, on average, required for a neutron of energy E_0 to be moderated to thermal energies, say 1 eV, can be estimated from

$$\langle \text{no. collisions} \rangle \simeq \frac{\ln[E_0(eV)/1.0]}{\xi} \tag{1.25}$$

The results are shown in Table 1.4 for $E_0 = 2$ MeV.

The parameter ξ, which is a measure of the moderating ability, decreases with nuclide mass, with the result that the number of collisions that are needed to moderate a fast neutron increases with nuclide mass. However, the effectiveness of a nuclide (or molecule) in moderating a neutron also depends on the relative probability that a collision will result in a scattering reaction, not a capture reaction, which would remove the neutron. Thus the parameter $\xi\Sigma_s/\Sigma_a$, referred to as the *moderating ratio*, is a measure of the effectiveness of a moderating material. Even though H_2O is the better moderator in terms of the number of collisions required to thermalize a fast neutron, D_2O is the more effective moderator because the absorption cross section for D is much less than that for H.

Example 1.2: Moderation by a Mixture. The moderating parameters for a mixture of isotopes is constructed by weighting the moderating parameters of the individual isotopes by their concentrations in the mixture. For example, in a mixture of ^{12}C and ^{238}U the average value of $\xi\Sigma_s = N_C\xi_C\sigma_{sC} + N_U\xi_U\sigma_{sU} = N_C(0.158)(2.3\times10^{-24}\ \text{cm}^2) + N_U(0.008)(4.8\times10^{-24}\ \text{cm}^2)$, where the fission spectrum range elastic scattering cross sections of Table 1.3 have been assumed to hold also in the

slowing-down range. The total absorption cross section is $\Sigma_a = N_C\sigma_{aC} + N_U\sigma_{aU} = N_C(0.002 \times 10^{-24}\ \text{cm}^2) + N_U(280 \times 10^{-24}\ \text{cm}^2)$ in the slowing-down range, where the resonance range cross sections from Table 1.3 have been used.

References

1 H. Cember, *Introduction to Health Physics*, 3rd ed., McGraw-Hill, New York (**1996**).

2 C. Nordborg and M. Salvatores, "Status of the JEF Evaluated Nuclear Data Library," *Proc. Int. Conf. Nuclear Data for Science and Technology*, Gatlinburg, TN, Vol. 2 (**1994**), p. 680.

3 R. W. Roussin, P. G. Young, and R. McKnight, "Current Status of ENDF/B-VI, *Proc. Int. Conf. Nuclear Data for Science and Technology*, Gatlinburg, TN, Vol. 2 (**1994**), p. 692.

4 Y. Kikuchi, "JENDL-3 Revision 2: JENDL 3-2," *Proc. Int. Conf. Nuclear Data for Science and Technology*, Gatlinburg, TN, Vol. 2 (**1994**), p. 685.

5 R. A. Knief, *Nuclear Engineering*, Taylor & Francis, Washington, DC (**1992**).

6 J. J. Schmidt, "Nuclear Data: Their Importance and Application in Fission Reactor Physics Calculations," in D. E. Cullen, R. Muranaka, and J. Schmidt, eds., *Reactor Physics Calculations for Applications in Nuclear Technology*, World Scientific, Singapore (**1990**).

7 A. Trkov, "Evaluated Nuclear Data Processing and Nuclear Reactor Calculations," in D. E. Cullen, R. Muranaka, and J. Schmidt, eds., *Reactor Physics Calculations for Applications in Nuclear Technology*, World Scientific, Singapore (**1990**).

8 *CINDA: An Index to the Literature on Microscopic Neutron Data*, International Atomic Energy Agency, Vienna; CINDA-A, 1935–1976 (**1979**); CINDA-B, 1977–1981 (**1984**); CINDA-89 (**1989**).

9 D. E. Cullen, "Nuclear Cross Section Preparation," in Y. Ronen, ed., *CRC Handbook of Nuclear Reactor Calculations I*, CRC Press, Boca Raton, FL (**1986**).

10 J. L. Rowlands and N. Tubbs, "The Joint Evaluated File: A New Nuclear Data Library for Reactor Calculations," *Proc. Int. Conf. Nuclear Data for Basic and Applied Science*, Santa Fe, NM, Vol. 2 (**1985**), p. 1493.

11 A. Calamand and H. D. Lemmel, *Short Guide to EXFOR*, IAEA-NDS-1, Rev. 3, International Atomic Energy Agency, Vienna (**1981**).

12 J. J. Duderstadt and L. G. Hamilton, *Nuclear Reactor Analysis*, Wiley, New York (**1976**), Chap. 2.

13 H. C. Honeck, *ENDF/B: Specifications for an Evaluated Data File for Reactor Applications*, USAEC report BNL-50066, Brookhaven National Laboratory, Upton, NY (**1966**).

14 I. Kaplan, *Nuclear Physics*, 2nd ed., Addison-Wesley, Reading, MA (**1963**).

15 L. J. Templin, ed., *Reactor Physics Constants*, 2nd ed., ANL-5800, Argonne National Laboratory, Argonne, IL (**1963**).

Problems

1.1. Demonstrate that the speeds of the neutron and nucleus in the CM system do not change in an elastic scattering event by using conservation of momentum and kinetic energy.

1.2. Estimate the probability that a 1-MeV neutron will be moderated to thermal without being captured in a mixture of uranium and water with $N_H/N_U = 1{:}1$. Repeat for a 1:1 mixture of uranium and carbon.

1.3. Neutrons are slowed down to thermal energies in a 1:1 mixture of H_2O and 4% enriched uranium (4%^{235}U, 96%^{238}U). Estimate the thermal value of $\eta = \nu\sigma_f/(\sigma_c + \sigma_f)$. Repeat the calculation for a mixture of (2%^{235}U, 2%^{239}Pu, 96%^{238}U).

1.4. Estimate the probability that a fission neutron will have a scattering collision with H_2O in the mixtures of Problem 1.3.

1.5. Calculate the average energy loss for neutrons at 1-MeV, 100-keV, 10-keV, and 1-keV scattering from carbon. Repeat the calculation for scattering from iron and from uranium.

1.6. Repeat Problem 1.5 for scattering from hydrogen and sodium.

1.7. Calculate the moderating ratio and the average number of collisions required to moderate a fission neutron to thermal for a 1:1 mixture of $^{12}C : ^{238}U$. Repeat for a 10:1 mixture.

1.8. Calculate the thermal absorption cross section for a 1:1 wt% mixture of carbon and 4% enriched uranium (e.g., 4%^{235}U, 96%^{238}U).

1.9. Derive Eq. (1.21) from Eqs. (1.20) and (1.19).

1.10. Calculate the average number of scattering events required to moderate a neutron's energy from above the resonance range to below the resonance range of ^{238}U for carbon, H_2O and D_2O moderators.